Measuring cosmology with Supernovae

Saul Perlmutter[1] and Brian P. Schmidt[2]

[1] Physics Division, Lawrence Berkeley National Laboratory, University of California, Berkeley, CA 94720, USA

[2] Research School of Astronomy and Astrophysics, The Australian National University, via Cotter Rd, Weston Creek, ACT 2611, Australia

Abstract. Over the past decade, supernovae have emerged as some of the most powerful tools for measuring extragalactic distances. A well developed physical understanding of type II supernovae allow them to be used to measure distances independent of the extragalactic distance scale. Type Ia supernovae are empirical tools whose precision and intrinsic brightness make them sensitive probes of the cosmological expansion. Both types of supernovae are consistent with a Hubble Constant within $\sim 10\%$ of $H_0 = 70$ km s^{-1} Mpc^{-1}. Two teams have used type Ia supernovae to trace the expansion of the Universe to a look-back time more than 60% of the age of the Universe. These observations show an accelerating Universe which is currently best explained by a cosmological constant or other form of dark energy with an equation of state near $w = p/\rho = -1$. While there are many possible remaining systematic effects, none appears large enough to challenge these current results. Future experiments are planned to better characterize the equation of state of the dark energy leading to the observed acceleration by observing hundreds or even thousands of objects. These experiments will need to carefully control systematic errors to ensure future conclusions are not dominated by effects unrelated to cosmology.

1 Introduction

Understanding the global history of the Universe is a fundamental goal of cosmology. One of the conceptually simplest tests in the repertoire of the cosmologist is observing how a standard candle dims as a function of redshift. The nearby Universe provides the current rate of expansion, and with more distant objects it is possible to start seeing the varied effects of cosmic curvature and the Universe's expansion history (usually expressed as the rate of acceleration/deceleration). Over the past several decades a paradigm for understanding the global properties of the Universe has emerged based on General Relativity with the assumption of a homogeneous and isotropic Universe. The relevant constants in this model are the Hubble constant (or current rate of cosmic expansion), the relative fractions of species of matter that contribute to the energy density of the Universe, and these species' equation of state.

Early luminosity distance investigations used the brightest objects available for measuring distance – bright galaxies [3,39], but these efforts were hampered by the impreciseness of the distance indicators and the changing properties of the distance indicators as a function of look back time. Although many other methods for measuring the global curvature and cosmic deceleration exist (see,

e.g., [66]), supernovae (SNe) have emerged as one of the preeminent distance methods due to their significant intrinsic brightness (which allows them to be observable in the distant Universe), ubiquity (they are visible in both the nearby and distant Universe), and their precision (type Ia SNe provide distances that have a precision of approximately 8%).

2   Supernovae as Distance Indicators

2.1   Type II Supernovae and the Expanding Photosphere Method

Massive stars come in a wide variety of luminosities and sizes and would seemingly not be useful objects for making distance measurements under the standard candle assumption. However, from a radiative transfer standpoint these objects are relatively simple and can be modeled with sufficient accuracy to measure distances to approximately 10%. The expanding photosphere method (EPM), was developed by Kirshner and Kwan [44], and implemented on a large number of objects by Schmidt et al. [86] after considerable improvement in the theoretical understanding of type II SN (SNII) atmospheres [15,16,99].

EPM assumes that SNII radiate as dilute blackbodies

$$\theta_{ph} = \frac{R_{ph}}{D} = \sqrt{\frac{F_\lambda}{\zeta^2 \pi B_\lambda(T)}}, \tag{1}$$

where θ_{ph} is the angular size of the photosphere of the SN, R_{ph} is the radius of the photosphere, D is the distance to the SN, F_λ is the observed flux density of the SN, and $B_\lambda(T)$ is the Planck function at a temperature T. Since SNII are not perfect blackbodies, we include a correction factor, ζ, which is calculated from radiate transfer models of SNII. SNe freely expand, and

$$R_{ph} = v_{ph}(t - t_0) + R_0, \tag{2}$$

where v_{ph} is the observed velocity of material at the position of the photosphere, and t is the time elapsed since the time of explosion, t_0. For most stars, the stellar radius ,R_0, at the time of explosion is negligible, and Eqs. (1–2) can be combined to yield

$$t = D \left(\frac{\theta_{ph}}{v_{ph}} \right) + t_0 \tag{3}$$

By observing a SNII at several epochs, measuring the flux density and temperature of the SN (via broad band photometry) and v_{ph} from the minima of the weakest lines in the SN spectrum, we can solve simultaneously for the time of explosion and distance to the SNII. The key to successfully measuring distances via EPM is an accurate calculation of $\zeta(T)$. Requisite calculations were performed by Eastman et al. [16] but, unfortunately, no other calculations of $\zeta(T)$ have yet been published for typical SNIIP progenitors.

Hamuy et al. [34] and Leonard et al. [52] have measured the distances to SN1999em, and they have investigated other aspects of EPM. Hamuy et al. [34] challenged the prescription of measuring velocities from the minima of weak lines and developed a framework of cross correlating spectra with synthesized spectra to estimate the velocity of material at the photosphere. This different prescription does lead to small systematic differences in estimated velocity using weak lines but, provided the modeled spectra are good representations of real objects, this method should be more correct. At present, a revision of the EPM distance scale using this method of estimating v_{ph} has not been made.

Leonard et al. [51] have obtained spectropolarimetry of SN1999em at many epochs and see polarization intrinsic to the SN which is consistent with the SN have asymmetries of $10-20\%$. Asymmetries at this level are found in most SNII [101], and may ultimately limit the accuracy EPM can achieve on a single object ($\sigma \sim 10\%$). However, the mean of all SNII distances should remain unbiased.

Type II SNe have played an important role in measuring the Hubble constant independent of the rest of the extragalactic distance scale. In the next decade it is quite likely that surveys will begin to turn up significant numbers of these objects at $z \sim 0.5$ and, therefore, the possibility exists that SNII will be able to make a contribution to the measurement of cosmological parameters beyond the Hubble Constant. Since SNII do not have the precision of the SNIa (next section) and are significantly harder to measure, they will not replace the SNIa but will remain an independent class of objects which have the potential to confirm the interesting results that have emerged from the SNIa studies.

2.2   Type Ia Supernovae as Standardized Candles

SNIa have been used as extragalactic distance indicators since Kowal [42] first published his Hubble diagram ($\sigma = 0.6$ mag) for type I SNe. We now recognize that the old type I SNe spectroscopic class is comprised of two distinct physical entities: SNIb/c which are massive stars that undergo core collapse (or in some rare cases might undergo a thermonuclear detonation in their cores) after losing their hydrogen atmospheres, and SNIa which are most likely thermonuclear explosions of white dwarfs. In the mid-1980s it was recognized that studies of the type I SN sample had been confused by these similar appearing SNe, which were henceforth classified as type Ib [59,94,102] and type Ic [36]. By the late 1980s/early 1990s, a strong case was being made that the vast majority of the true type Ia SNe had strikingly similar light curve shapes [11,46–48], spectral time series [6,18,28,62], and absolute magnitudes [47,54]. There were a small minority of clearly peculiar type Ia SNe (e.g., SN1986G [63], SN1991bg [19,49], and SN1991T [19,78]), but these could be identified and removed by their unusual spectral features. A 1992 review by Branch and Tammann [7] of a variety of studies in the literature concluded that the intrinsic dispersion in B and V maximum for type Ia SNe must be < 0.25 mag, making them "the best standard candles known so far."

In fact, the Branch and Tammann review indicated that the magnitude dispersion was probably even smaller, but the measurement uncertainties in the

available datasets were too large to tell. The *Calan/Tololo Supernova Search (CTSS)*, a program begun by Hamuy et al. [31] in 1990, took the field a dramatic step forward by obtaining a crucial set of high quality SN light curves and spectra. By targeting a magnitude range that would discover type Ia SNe in the redshift range $z = 0.01 - 0.1$, the *CTSS* was able to compare the peak magnitudes of SNe whose relative distance could be deduced from their Hubble velocities.

The *CTSS* observed some 25 fields (out of a total sample of 45 fields) twice a month for over three and one half years with photographic plates or film at the *Cerro Tololo Inter-American Observatory (CTIO)* Curtis Schmidt telescope, and then organized extensive follow-up photometry campaigns primarily on the *CTIO* 0.9 m telescope, and spectroscopic observation on either the *CTIO* 4 m or 1.5 m telescope. Toward the end of this search, Hamuy et al. [31] pointed out the difficulty of this comprehensive project: "Unfortunately, the appearance of a SN is not predictable. As a consequence of this we cannot schedule the followup observations *a priori*, and we generally have to rely on someone else's telescope time. This makes the execution of this project somewhat difficult." Despite these challenges, the search was a major success; with the cooperation of many visiting *CTIO* astronomers and *CTIO* staff, it contributed 30 new type Ia SN light curves to the pool [32] with an almost unprecedented control of measurement uncertainties.

As the *CTSS* data began to become available, several methods were presented that could select for the "most standard" subset of the type Ia standard candles, a subset which remained the dominant majority of the ever-growing sample [8]. For example, Vaughan et al. [97] presented a cut on the B-V color at maximum that would select what were later called the "Branch Normal" SNIa, with an observed dispersion of less than 0.25 mag.

Phillips [64] found a tight correlation between the rate at which a type Ia SN's luminosity declines and its absolute magnitude, a relation which apparently applied not only to the Branch Normal type Ia SNe, but also to the peculiar type Ia SNe. Phillips plotted the absolute magnitude of the existing set of nearby SNIa, which had dense photoelectric or CCD coverage, versus the parameter $\Delta m_{15}(B)$, the amount the SN decreased in brightness in the B-band over the 15 days following maximum light. The sample showed a strong correlation which, if removed, dramatically improved the predictive power of SNIa. Hamuy et al. [33] used this empirical relation to reduce the scatter in the Hubble diagram to $\sigma < 0.2$ mag in V for a sample of nearly 30 SNIa from the *CTSS* search.

Impressed by the success of the $\Delta m_{15}(B)$ parameter, Riess et al. [79] developed the *multi-color light curve shape method (MLCS)*, which parameterized the shape of SN light curves as a function of their absolute magnitude at maximum. This method also included a sophisticated error model and fitted observations in all colors simultaneously, allowing a color excess to be included. This color excess, which we attribute to intervening dust, enabled the extinction to be measured. Another method that has been used widely in cosmological measurements with SNIa is the "stretch" method described in Perlmutter et al. [74,77]. This

method is based on the observation that the entire range of SNIa light curves, at least in the B and V-bands, can be represented with a simple time stretching (or shrinking) of a canonical light curve. The coupled stretched B and V light curves serve as a parameterized set of light curve shapes [26], providing many of the benefits of the MLCS method but as a much simpler (and constrained) set. This method, as well as recent implementations of Δm_{15}(B) [24,65], also allows extinction to be directly incorporated into the SNIa distance measurements. Other methods that correct for intrinsic luminosity differences or limit the input sample by various criteria have also been proposed to increase the precision of type Ia SNe as distance indicators [9,17,93,95]. While these latter techniques are not as developed as the Δm_{15}(B), *MLCS*, and stretch methods, they all provide distances that are comparable in precision, roughly $\sigma = 0.18$ mag about the inverse square law, equating to a fundamental precision of SNIa distances of $\sim 6\%$ (0.12 mag), once photometric uncertainties and peculiar velocities are removed. Finally, a "poor man's" distance indicator, the snapshot method [80], combines information contained in one or more SN spectra with as little as one night's multi-color photometry. This method's accuracy depends critically on how much information is available.

3   Cosmological Parameters

The standard model for describing the global evolution of the Universe is based on two equations that make some simple, and hopefully valid, assumptions. If the Universe is isotropic and homogenous on large scales, the Robertson-Walker Metric,

$$ds^2 = dt^2 - a(t) \left[\frac{dr^2}{1 - kr^2} + r^2 d\theta^2 \right].$$

(4)

gives the line element distance(s) between two objects with coordinates r,θ and time separation, t. The Universe is assumed to have a simple topology such that, if it has negative, zero, or positive curvature, k takes the value $-1, 0, 1$, respectively. These models of the Universe are said to be open, flat, or closed, respectively. The dynamic evolution of the Universe needs to be input into the Robertson-Walker Metric by the specification of the scale factor $a(t)$, which gives the radius of curvature of the Universe over time – or more simply, provides the relative size of a piece of space at any time. This description of the dynamics of the Universe is derived from General Relativity, and is known as the Friedman equation

$$H^2 \equiv (\dot{a}/a)^2 = \frac{8\pi G\rho}{3} - \frac{k}{a^2}.$$

(5)

The expansion rate of our Universe (H), is called the Hubble parameter (or the Hubble constant, H_0, at the present epoch) and depends on the content of the Universe. Here we assume the Universe is composed of a set of components, each having a fraction, Ω_i, of the critical density

$$\Omega_i = \frac{\rho_i}{\rho_{crit}} = \frac{\rho_i}{\frac{3H_0^2}{8\pi G}}, \tag{6}$$

with an equation of state which relates the density, ρ_i, and pressure, p_i, as $w_i = p_i/\rho_i$. For example, w_i takes the value 0 for normal matter, $+1/3$ for photons, and -1 for the cosmological constant. The equation of state parameter does not need to remain fixed; if scalar fields are present, the effective w will change over time. Most reasonable forms of matter or scalar fields have $w_i \geq -1$, although nothing seems manifestly forbidden. Combining Eqs. (4–6) yields solutions to the global evolution of the Universe [13].

The luminosity distance, D_L, which is defined as the apparent brightness of an object as a function of its redshift z – the amount an object's light has been stretched by the expansion of the Universe – can be derived from Eqs. (4–6) by solving for the surface area as a function of z, and taking into account the effects of time dilation [25,26,50,82] and energy dimunition as photons get stretched traveling through the expanding Universe. D_L is given by the numerically integrable equation,

$$D_L = \frac{c}{H_0}(1+z)\kappa_0^{-1/2}S\{\kappa_0^{1/2}\int_0^z dz'[\sum_i \Omega_i(1+z')^{3+3w_i} - \kappa_0(1+z')^2]^{-1/2}\}. \tag{7}$$

$S(x) = \sin(x)$, x, or $\sinh(x)$ for closed, flat, and open models respectively, and the curvature parameter κ_0, is defined as $\kappa_0 = \sum_i \Omega_i - 1$.

Historically, Eq. (7) has not been easily integrated and has been expanded in a Taylor series to give

$$D_L = \frac{c}{H_0}\{z + z^2\left(\frac{1-q_0}{2}\right) + \mathcal{O}(z^3)\}, \tag{8}$$

where the deceleration parameter, q_0, is given by

$$q_0 = \frac{1}{2}\sum_i \Omega_i(1+3w_i). \tag{9}$$

From Eq. (9) we can see that, in the nearby Universe, the luminosity distances scale linearly with redshift, with H_0 serving as the constant of proportionality. In the more distant Universe, D_L depends to first order on the rate of acceleration/deceleration (q_0) or, equivalently, on the amount and types of matter that make up the Universe. For example, since normal matter has $w_M = 0$ and the cosmological constant has $w_\Lambda = -1$, a universe composed of only these two forms of matter/energy has $q_0 = \Omega_M/2 - \Omega_\Lambda$. In a universe composed of these two types of matter, if $\Omega_\Lambda < \Omega_M/2$, q_0 is positive and the universe is decelerating. These decelerating universes have D_L smaller as a function of z than their accelerating counterparts.

If distance measurements are made at a low-z and a small range of redshift at higher z (e.g., $0.3 > z > 0.5$), there is a degeneracy between Ω_M and Ω_Λ.
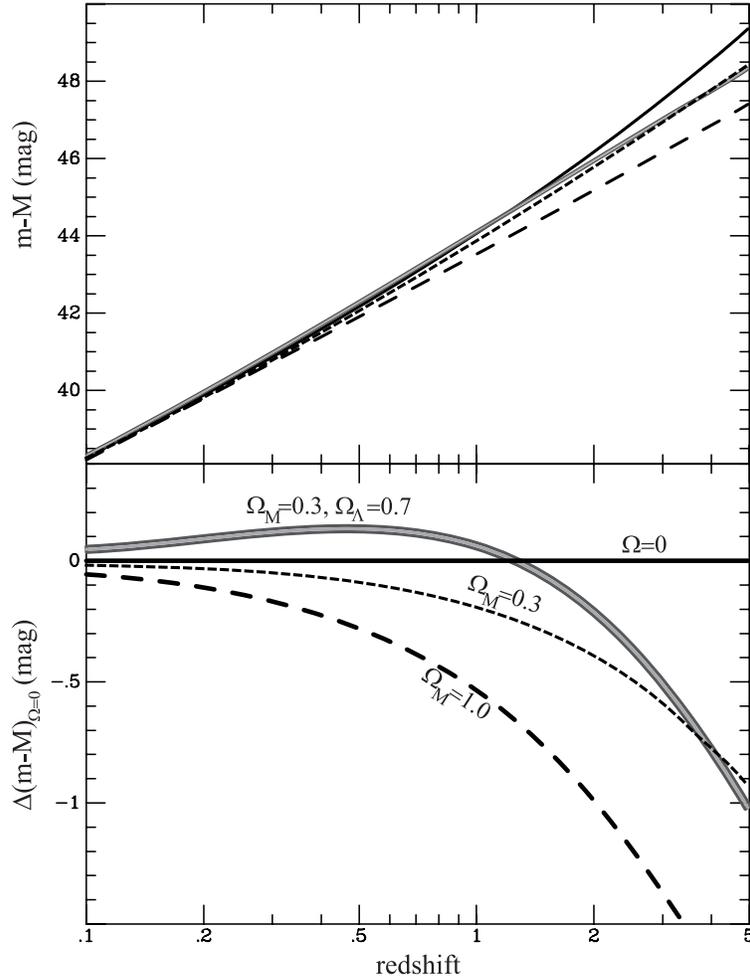
Fig. 1. D_L expressed as distance modulus $(m - M)$ for four relevant cosmological models; $\Omega_M = 0$, $\Omega_\Lambda = 0$ (empty Universe, *solid line*); $\Omega_M = 0.3$, $\Omega_\Lambda = 0$ (*short dashed line*); $\Omega_M = 0.3$, $\Omega_\Lambda = 0.7$ (*hatched line*); and $\Omega_M = 1.0$, $\Omega_\Lambda = 0$ (*long dashed line*). In the bottom panel the empty Universe has been subtracted from the other models to highlight the differences.

It is impossible to pin down the absolute amount of either species of matter. One can only determine their relative dominance, which, at $z = 0$, is given by Eq. (9). However, Goobar and Perlmutter [27] pointed out that by observing objects over a larger range of high redshift (e.g., $0.3 > z > 1.0$) this degeneracy can be broken, providing a measurement of the absolute fractions of Ω_M and Ω_Λ.

To illustrate the effect of cosmological parameters on the luminosity distance, in Fig. 1 we plot a series of models for both Λ and non-Λ universes. In the top
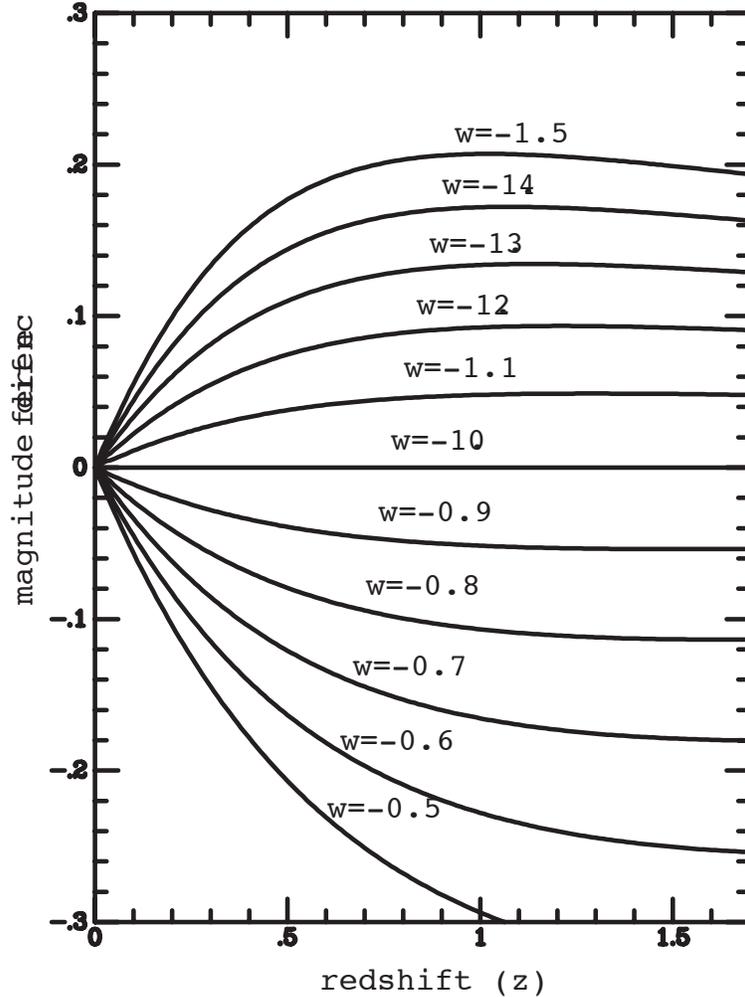
Fig. 2. D_L for a variety of cosmological models containing $\Omega_M = 0.3$ and $\Omega_x = 0.7$ with a constant (not time-varying) equation of state w_x. The $w_x = -1$ model has been subtracted off to highlight the differences between the various models

panel, the various models show the same linear behavior at $z < 0.1$ with models having the same H_0 being indistinguishable to a few percent. By $z = 0.5$ the models with significant Λ are clearly separated, with luminosity distances that are significantly further than the zero-Λ universes. Unfortunately, two perfectly reasonable universes, given our knowledge of the local matter density of the Universe ($\Omega_M \sim 0.2$), one with a large cosmological constant, $\Omega_\Lambda = 0.7$, $\Omega_M = 0.3$ and one with no cosmological constant, $\Omega_M = 0.2$, show differences of less than 25%, even to redshifts of $z > 5$. Interestingly, the maximum difference between the two models is at $z \sim 0.8$, not at large z. Fig. 2 illustrates the effect

of changing the equation of state of the non-matter, dark energy component, assuming a flat universe, $\Omega_{tot} = 1$. If we are to discern a dark energy component that is not a cosmological constant, measurements better than 5% are clearly required, especially since the differences in this diagram include the assumption of flatness and also fix the value of Ω_M. In fact, to discriminate among the full range of dark energy models with time varying equations of state will require much better accuracy than even this challenging goal.

4   Measuring the Hubble Constant

Schmidt et al. [86], using a sample of 16 SNII, estimated $H_0 = 73\pm6$(statistical)±7 (systematic) using EPM. This estimate is independent of other rungs in the extragalactic distance ladder, the most important of which are the Cepheids, which currently calibrate most other distance methods (such as SNIa). The Cepheid and EPM distance scales, compared galaxy to galaxy, agree to within 5% and are consistent within the errors [16,52]. This provides confidence that both methods are providing accurate distances.

The current nearby SNIa sample [24,32,41,84] contains more than 100 objects (Fig. 3), and accurately defines the slope in the Hubble diagram from $0 < z < 0.1$ to 1%. To measure H_0, SNIa must still be externally calibrated with Cepheids, and this calibration is the major limitation to measuring H_0 with SNIa. Two separate teams have analyzed the Cepheids and SNIa but have obtained divergent values for the Hubble constant. Saha et al. [88] find $H_0 = 59 \pm 6$, whereas Freedman et al. [20] find $H_0 = 71 \pm 2 \pm$ (6 systematic). Of the 12 SNIa for which there are Cepheid distances to the host galaxy (SN1895B*, SN1937C*, SN1960F*, SN1972E, SN1974G*, SN1981B, SN1989B, SN1990N, SN1991T, SN1998eq, SN1998bu, and SN1999by), four were observed by non-digital means (marked by *) and are best excluded from analysis on the grounds that non-digital photometry routinely has systematic errors far greater than 0.1 mag. Jha [41] has compared the SNIa distances using an updated version of *MLCS* to the Cepheid host galaxy distances measured by the two *Hubble Space Telescope (HST)* teams. Using only the digitally observed SNIa, he finds, using distances from the SNIa project of Saha et al. [88], $H_0 = 66 \pm 3 \pm$ (7 systematic) km s^{-1} Mpc^{-1}. Applying the same analysis to the Key Project distances by Freedman et al. [20] gives $H_0 = 76 \pm 3 \pm$ (8 systematic) km s^{-1} Mpc^{-1}. This difference is not due to SNIa errors, but rather to the different ways the two teams have measured Cepheid distances with *HST*. The two values do overlap when the systematic uncertainties are included, but it is still uncomfortable that the discrepancies are so large, particularly when some systematic uncertainties are common between the two teams.

At present, SNe provide the most convincing constraints with $H_0 \sim 70 \pm 10$ km s^{-1} Mpc^{-1}. However, future work on measuring H_0 lies not with the SNe but with the Cepheid calibrators, or possibly in using other primary distance indicators such as EPM or the Sunyaev-Zeldovich effect.
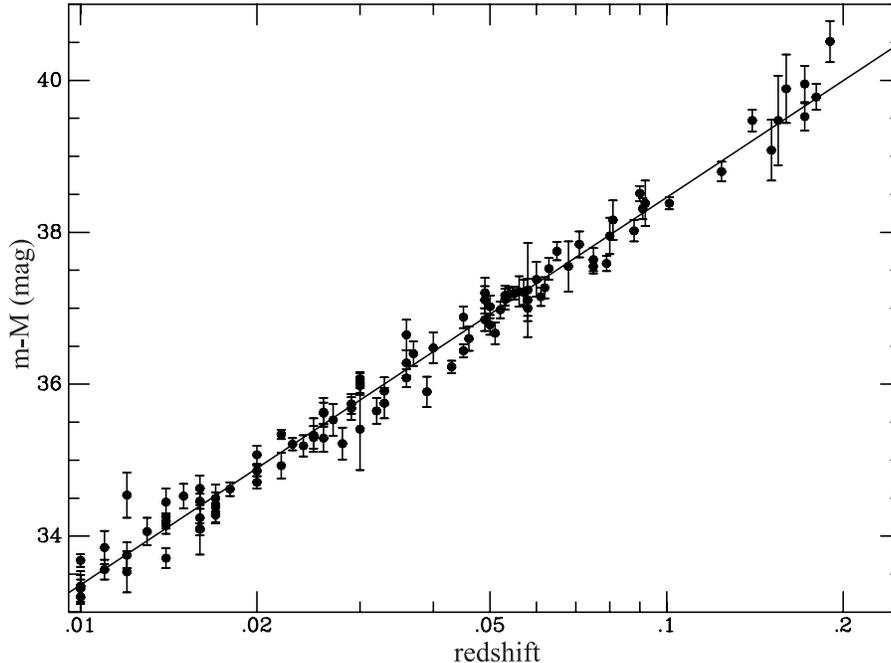
Fig. 3. The Hubble diagram for SNIa from $0.01 > z > 0.2$ [24,33,41,84]. The 102 objects in this range have a residual about the inverse square line of $\sim 10\%$.

5   The Measurement of Acceleration

The intrinsic brightness of SNIa allow them to be discovered to $z > 1.5$ with current instrumentation (while a comparably deep search for type II SNe would only reach redshifts of $z \sim 0.5$). In the 1980s, however, finding, identifying, and studying even the impressively luminous type Ia SNe was a daunting challenge, even towards the lower end of the redshift range shown in Fig. 1. At these redshifts, beyond $z \sim 0.25$, Fig. 1 shows that relevant cosmological models could be distinguished by differences of order 0.2 mag in their predicted luminosity distances. For SNIa with a dispersion of 0.2 mag, 10 well observed objects should provide a 3σ separation between the various cosmological models. It should be noted that the uncertainty described above in measuring H_0 is not important in measuring the parameters for different cosmological models. Only the relative brightness of objects near and far is being exploited in Eq. (7) and the absolute value of H_0 scales out.

The first distant SN search was started by the Danish team of Nørgaard-Nielsen et al. [57]. With significant effort and large amounts of telescope time spread over more than two years, they discovered a single SNIa in a $z = 0.3$ cluster of galaxies (and one SNII at $z = 0.2$) [35,57]. The SNIa was discovered well after maximum light on an observing night that could not have been predicted, and was only marginally useful for cosmology. However, it showed that

such high redshift SNe did exist and could be found, but that they would be very difficult to use as cosmological tools.

Just before this first discovery in 1988, a search for high redshift type Ia SNe using a then novel wide field camera on a much larger (4m) telescope was begun at the *Lawrence Berkeley National Laboratory (LBNL)* and the *Center for Particle Astrophysics*, at Berkeley. This search, now known as the *Supernova Cosmological Project (SCP)*, was inspired by the impressive studies of the late 1980s indicating that extremely similar type Ia SN events could be recognized by their spectra and light curves, and by the success of the *LBNL* fully robotic low-redshift SN search in finding 20 SNe with automatic image analysis [56,67].

The *SCP* targeted a much higher redshift range, $z > 0.3$, in order to measure the (presumed) deceleration of the Universe, so it faced a different challenge than the *CTSS* search. The high redshift SNe required discovery, spectroscopic confirmation, and photometric follow up on much larger telescopes. This precious telescope time could neither be borrowed from other visiting observers and staff nor applied for in sufficient quantities spread throughout the year to cover all SNe discovered in a given search field, and with observations early enough to establish their peak brightness. Moreover, since the observing time to confirm high redshift SNe was significant on the largest telescopes, there was a clear "chicken and egg" problem: telescope time assignment committees would not award follow-up time for a SN discovery that might, or might not, happen on a given run (and might, or might not, be well past maximum) and, without the follow-up time, it was impossible to demonstrate that high redshift SNe were being discovered by the *SCP*.

By 1994, the *SCP* had solved this problem, first by providing convincing evidence that SNe, such as SN1992bi, could be discovered near maximum (and K-corrected) out to $z = 0.45$ [73], and then by developing and successfully demonstrating a new observing strategy that could effectively guarantee SN discoveries on a predetermined date, all before or near maximum light [70–72,76]. Instead of discovering a single SN at a time on average (with some runs not finding one at all), the new approach aimed to discover an entire "batch" of half-a-dozen or more type Ia SNe at a time by observing a much larger number of galaxies in a single two or three day period a few nights before new Moon. By comparing these observations with the same observations taken towards the end of dark time almost three weeks earlier, it was possible to select just those SNe that were still on the rise or near maximum. The chicken and egg problem was solved, and now the follow-up spectroscopy and photometry could be applied for and scheduled on a pre-specified set of nights. The new strategy worked – the *SCP* discovered batches of high redshift SNe,and no one would ever again have to hunt for high-redshift SNe without the crucial follow-up scheduled in advance.

The *High-Z SN Search (HZSNS)* was conceived at the end of 1994, when this group of astronomers became convinced that it was both possible to discover SNIa in large numbers at $z > 0.3$ by the efforts of Perlmutter et al.[70–72], and also use them as precision distance indicators as demonstrated by the *CTSS*

group [32]. Since 1995, the *SCP* and *HZSNS* have both worked avidly to obtain a significant set of high redshift SNIa.

5.1   Discovering SNIa

The two high redshift teams both used this pre-scheduled discovery and follow-up batch strategy. They each aimed to use the observing resources they had available to best scientific advantage, choosing, for example, somewhat different exposure times or filters.

Quantitatively, type Ia SNe are rare events on an astronomer's time scale – they occur in a galaxy like the Milky Way a few times per millennium (see, e.g., [12,60,61] and the chapter by Cappellaro in this volume). With modern instruments on 4 meter-class telescopes, which observe 1/3 of a square degree to R = 24 mag in less than 10 minutes, it is possible to search a million galaxies to $z < 0.5$ for SNIa in a single night.

Since SNIa take approximately 20 days to rise from undetectable to maximum light [81], the three-week separation between observing periods (which equates to 14 rest frame days at $z = 0.5$) is a good filter to catch the SNe on the rise. The SNe are not always easily identified as new stars on the bright background of their host galaxies, so a relatively sophisticated process must be used to identify them. The process, which involves 20 Gigabytes of imaging data per night, consists of aligning a previous epoch, matching the image star profiles (through convolution), and scaling the two epochs to make the two images as identical as possible. The difference between these two images is then searched for new objects which stand out against the static sources that have been largely removed in the differencing process [73,74,76,87]. The dramatic increase in computing power in the 1980s was an important element in the development of this search technique, as was the construction of wide-field cameras with ever larger CCD detectors or mosaics of such detectors [104].

This technique is very efficient at producing large numbers of objects that are, on average, at or near maximum light, and does not require unrealistic amounts of large telescope time. It does, however, place the burden of work on follow-up observations, usually with different instruments on different telescopes. With the large number of objects discovered (50 in two nights being typical), a new strategy is being adopted by both the *SCP* and *HZSNS* teams, as well as additional teams like the *Canada France Hawaii Telescope (CFHT)* legacy survey, where the same fields are repeatedly scanned several times per month, in multiple colors, for several consecutive months. This type of observing program provides both discovery of new objects and their follow up, all integrated into one efficient program. It does require a large block of time on a single telescope – a requirement which was not politically feasible in years past, but is now possible.

5.2   Obstacles to Measuring Luminosity Distances at High-*Z*

As shown above, the distances measured to SNIa are well characterized at $z < 0.1$, but comparing these objects to their more distant counterparts requires great

care. Selection effects can introduce systematic errors as a function of redshift, as can uncertain K-corrections and a possible evolution of the SNIa progenitor population as a function of look-back time. These effects, if they are large and not constrained or corrected, will limit our ability to accurately measure relative luminosity distances, and have the potential to reduce the efficacy of high-z type Ia SNe for measuring cosmology [74,77,83,87].

K-Corrections: As SNe are observed at larger and larger redshifts, their light is shifted to longer wavelengths. Since astronomical observations are normally made in fixed band passes on Earth, corrections need to be applied to account for the differences caused by the spectrum shifting within these band passes. These corrections take the form of integrating the spectrum of an SN over the relevant band passes, shifting the SN spectrum to the correct redshift, and re-integrating. Kim et al. [43] showed that these effects can be minimized if one does not use a single bandpass, but instead chooses the bandpass closest to the redshifted rest-frame bandpass, as they had done for SN1992bi [73]. They showed that the inter-band K-correction is given by

$$K_{ij}(z) = 2.5 \log \left[(1+z) \frac{\int F(\lambda) S_i(\lambda) d\lambda}{\int F(\lambda/(1+z)) S_j(\lambda) d\lambda} \frac{\int Z(\lambda) S_j(\lambda) d\lambda}{\int Z(\lambda) S_i(\lambda) d\lambda} \right], \qquad (10)$$

where $K_{ij}(z)$ is the correction to go from filter i to filter j, and $Z(\lambda)$ is the spectrum corresponding to zero magnitude of the filters.

The brightness of an object expressed in magnitudes, as a function of z is

$$m_i(z) = 5 \log \left[\frac{D_L(z)}{\mathrm{Mpc}} \right] + 25 + M_j + K_{ij}(z), \qquad (11)$$

where $D_L(z)$ is given by Eq. (7), M_j is the absolute magnitude of object in filter j, and K_{ij} is given by Eq. (10). For example, for $H_0 = 70$ km s^{-1} Mpc^{-1}, and $D_L = 2835$ Mpc ($\Omega_M = 0.3, \Omega_\Lambda = 0.7$), at maximum light a SNIa has $M_B = -19.5$ mag and a $K_{BR} = -0.7$ mag. We therefore expect an SNIa at $z = 0.5$ to peak at $m_R \sim 22.1$ mag for this set of cosmological parameters.

K-correction errors depend critically on three uncertainties:

1. Accuracy of spectrophotometry of SNe. To calculate the K-correction, the spectra of SNe are integrated in Eq. (10). These integrals are insensitive to a grey shift in the flux calibration of the spectra, but any wavelength dependent flux calibration error will translate into erroneous K-corrections.
2. Accuracy of the absolute calibration of the fundamental astronomical standard systems. Eq. (10) shows that the K-corrections are sensitive to the shape of the astronomical band passes and to the zero points of these band passes.
3. Accuracy of the choice of SNIa spectrophotometry template used to calculate the corrections. Although a relatively homogenous class, there are variations in the spectra of SNIa. If a particular object has, for example, a stronger

calcium triplet than the average SNIa, the K-corrections will be in error unless an appropriate subset of SNIa spectra are used in the calculations.

The first error should not be an issue if correct observational procedures are used on an instrument that has no fundamental problems. The second error is currently estimated to be small (~ 0.01 mag), based on the consistency of spectrophotometry and broadband photometry of the fundamental standards, Sirius and Vega [5]. To improve this uncertainty will require new, careful experiments to accurately calibrate a star, such as Vega or Sirius (or a White Dwarf or solar analog star), and to carefully infer the standard bandpass that defines the photometric system in use at telescopes. The third error requires a large database to match as closely as possible an SN with the spectrophotometry used to calculate the K-corrections. Nugent et al. [58] have shown that extinction and color are related and, by correcting the spectra to force them to match the photometry of the SN needing K-corrections, that it is possible to largely eliminate errors 1 and 3, even when using spectra that are not exact matches (in epoch or in fine detail) to the SNIa being K-corrected. Scatter in the measured K-corrections from a variety of telescopes and objects allows us to estimate the combined size of the effect for the first and third errors. These appear to be ~ 0.01 mag for redshifts where the high-z and low-z filters have a large region of overlap (e.g., R-band matched to B-band at $z = 0.5$).

Extinction: In the nearby Universe we see SNIa in a variety of environments, and about 10% have significant extinction [30]. Since we can correct for extinction by observing two or more wavelengths, it is possible to remove any first order effects caused by a changing average extinction of SNIa as a function of z. However, second order effects, such as possible evolution of the average properties of intervening dust, could still introduce systematic errors. This problem can also be addressed by observing distant SNIa over a decade or so of wavelength in order to measure the extinction law to individual objects. Unfortunately, this is observationally very expensive. Current observations limit the total systematic effect to < 0.06 mag, as most of our current data is based on two color observations.

An additional problem is the existence of a thin veil of dust around the Milky Way. Measurements from the *Cosmic Background Explorer (COBE)* satellite accurately determined the relative amount of dust around the Galaxy [89], but there is an uncertainty in the absolute amount of extinction of about $2 - 3\%$. This uncertainty is not normally a problem, since it affects everything in the sky more or less equally. However, as we observe SNe at higher and higher redshifts, the light from the objects is shifted to the red and is less affected by the Galactic dust. Our present knowledge indicates that a systematic error as large as 0.06 mag is attributable to this uncertainty.

Selection Effects: As we discover SNe, we are subject to a variety of selection effects, both in our nearby and distant searches. The most significant effect is the

Malmquist Bias – a selection effect which leads magnitude limited searches to find brighter than average objects near their distance limit since brighter objects can be seen in a larger volume than their fainter counterparts. Malmquist Bias errors are proportional to the square of the intrinsic dispersion of the distance method, and because SNIa are such accurate distance indicators these errors are quite small, ~ 0.04 mag. Monte Carlo simulations can be used to estimate such selection effects, and to remove them from our data sets [74,76,77,87]. The total uncertainty from selection effects is ~ 0.01 mag and, interestingly, may be worse for lower redshift objects because they are, at present, more poorly quantified.

Gravitational Lensing: Several authors have pointed out that the radiation from any object, as it traverses the large scale structure between where it was emitted and where it is detected, will be weakly lensed as it encounters fluctuations in the gravitational potential [37,45,100]. On average, most of the light travel paths go through under-dense regions and objects appear de-magnified. Occasionally, the light path encounters dense regions and the object becomes magnified. The distribution of observed fluxes for sources is skewed by this process such that the vast majority of objects appear slightly fainter than the canonical luminosity distance, with the few highly magnified events making the mean of all light paths unbiased. Unfortunately, since we do not observe enough objects to capture the entire distribution, unless we know and include the skewed shape of the lensing a bias will occur. At $z = 0.5$, this lensing is not a significant problem: If the Universe is flat in normal matter, the large scale structure can induce a shift of the mode of the distribution by only a few percent. However, the effect scales roughly as z^2, and by $z = 1.5$ the effect can be as large as 25% [38]. While corrections can be derived by measuring the distortion of background galaxies near the line of sight to each SN, at $z > 1$, this problem may be one which ultimately limits the accuracy of luminosity distance measurements, unless a large enough sample of SNe at each redshift can be used to characterize the lensing distribution and average out the effect. For the $z \sim 0.5$ sample, the error is < 0.02 mag, but it is much more significant at $z > 1$ (e.g., for SN1997ff) [4,55], especially if the sample size is small.

Evolution: SNIa are seen to evolve in the nearby Universe. Hamuy et al. [29] plotted the shape of the SN light curves against the type of host galaxy. SNe in early hosts (galaxies without recent star formation) consistently show light curves which rise and fade more quickly than SNe in late-type hosts (galaxies with on-going star formation). However, once corrected for light curve shape the luminosity shows no bias as a function of host type. This empirical investigation provides reassurance for using SNIa as distance indicators over a variety of stellar population ages. It is possible, of course, to devise scenarios where some of the more distant SNe do not have nearby analogues, so as supernovae are studied at increasingly higher redshifts it can become important to obtain detailed spectroscopic and photometric observations of every distant SN to recognize and reject examples that have no nearby analogues.

In principle, it should be possible to use differences in the spectra and light curves between nearby and distant SNe, combined with theoretical modeling, to correct any differences in absolute magnitude. Unfortunately, theoretical investigations are not yet advanced enough to precisely quantify the effect of these differences on the absolute magnitude. A different, empirical approach to handle SN evolution [10] is to divide the SNe into subsamples of very closely matched events, based on the details of the their light curves, spectral time series, host galaxy properties, etc. A separate Hubble diagram can then be constructed for each subsample of SNe, and each will yield an independent measurement of the cosmological parameters. The agreement (or disagreement) between the results from the separate subsamples is an indicator of the total effect of evolution. A simple, first attempt at this kind of test has been performed by comparing the results for SNe found in elliptical host galaxies to SNe found in late spirals or irregular hosts, and the cosmological results from these subsamples were found to agree well [91].

Finally, it is possible to move to higher redshifts and see if the SNe deviate from the predictions of Eq. (7). At a gross level, we expect an accelerating Universe to be decelerating in the past because the matter density of the Universe increases with redshift, whereas the density of any dark energy leading to acceleration will increase at a slower rate than this (or not at all in the case of a cosmological constant). If the observed acceleration is caused by some sort of systematic effect, it is likely to continue to increase (or at least remain steady) with z, rather than disappear like the effects of dark energy. A first comparison has been made with SN1997ff at $z \sim 1.7$ [85], and it seems consistent with a decelerating Universe at that epoch. More objects are necessary for a definitive answer, and these should be provided by several large programs that have been discovering such type Ia SNe at the *W.M. Keck Telescope I (KECK I)*, *Subaru Telescope)*, and *HST* telescopes.

5.3   High Redshift SNIa Observations

The *SCP* [74] in 1997 presented their first results with 7 objects at a redshift around $z = 0.4$. These objects hinted at a decelerating Universe with a measurement of $\Omega_M = 0.88^{+0.69}_{-0.60}$, but were not definitive. Soon after, the *SCP* published a further result, with a $z \sim 0.84$ SNIa observed with the *KECK I* and *HST* added to the sample [75], and the *HZSNS* presented the results from their first four objects [22,87]. The results from both teams now ruled out a $\Omega_M = 1$ Universe with greater than 95% significance. These findings were again superceded dramatically when both teams announced results including more SNe (10 more *HZSNS* SNe, and 34 more *SCP* SNe) that showed not only were the SN observations incompatible with a $\Omega_M = 1$ Universe, they were also incompatible with a Universe containing only normal matter [77,83]. Fig. 4 shows the Hubble diagram for both teams. Both samples show that SNe are, on average, fainter than would be expected, even for an empty Universe, indicating that the Universe is accelerating. The agreement between the experimental results of the two teams
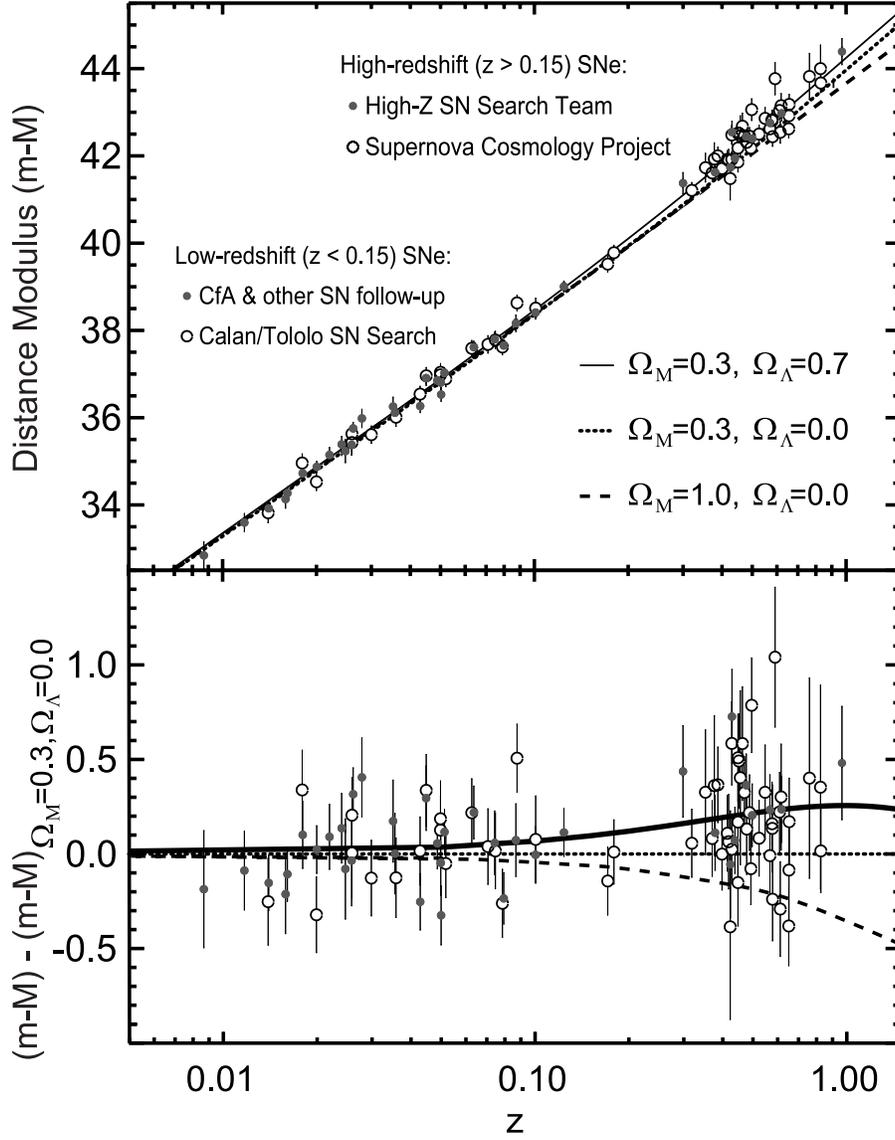
Fig. 4. *Upper panel:* The Hubble diagram for high redshift SNIa from both the *HZSNS* [83] and the *SCP* [77]. *Lower panel:* The residual of the distances relative to a $\Omega_M = 0.3$, $\Omega_\Lambda = 0.7$ Universe. The $z < 0.15$ objects for both teams are drawn from *CTSS* sample [32], so many of these objects are in common between the analyses of the two teams.
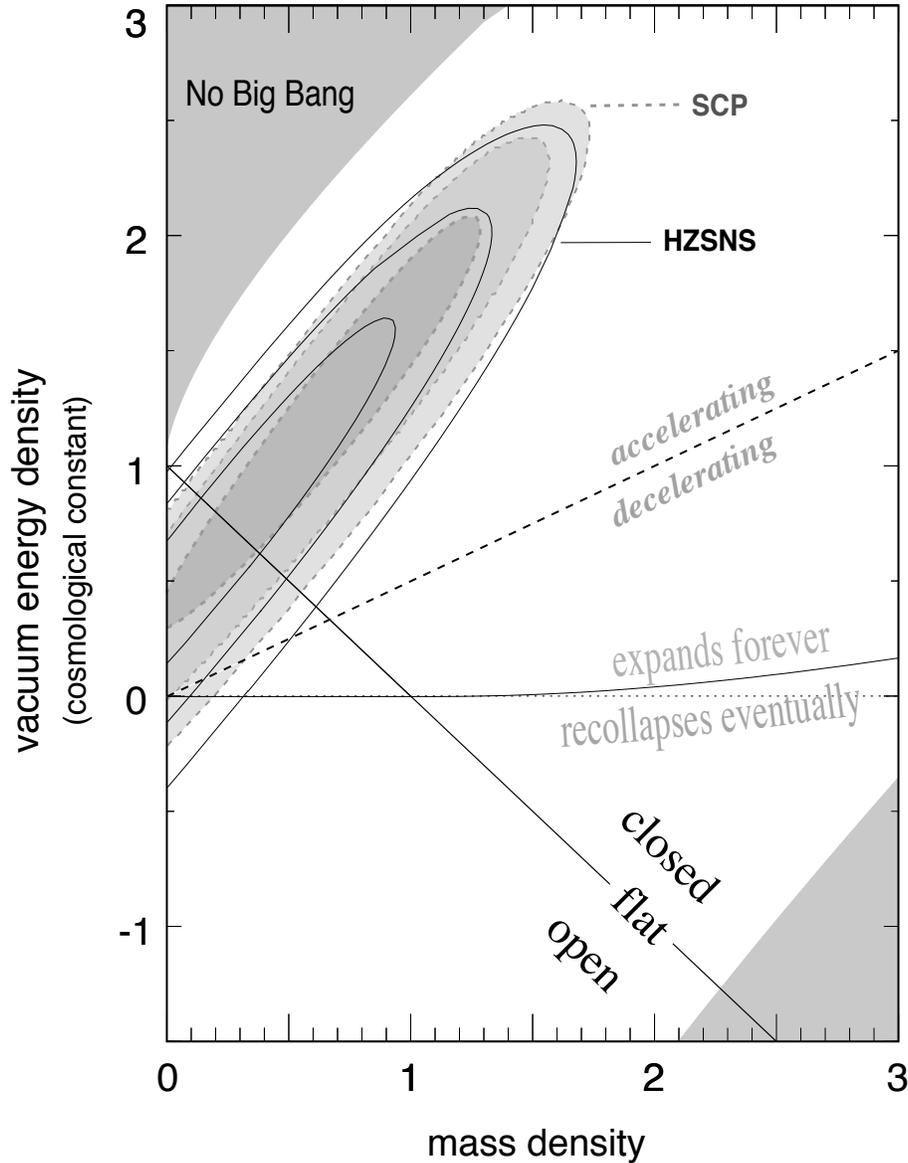
Fig. 5. The confidence regions for both *HZSNS* [83] and *SCP* [77] for Ω_M, Ω_Λ. The two experiments show, with remarkable consistency, that $\Omega_\Lambda > 0$ is required to reconcile observations and theory. The *SCP* result is based on measurements of 42 distant SNIa. (The analysis shown here is uncorrected for host galaxy extinction;see [77] for the alternative analyses with host extinction correction, which is shown to make little difference in this data set.) The *HZSNS* result is based on measurements of 16 SNIa, including 6 snapshot distances [80], of which two are *SCP* SNe from the 42 SN sample. The $z < 0.15$ objects used to constrain the fit for both teams are drawn from the *CTSS* sample [32], so many of these objects are common between the analyses by the two teams.
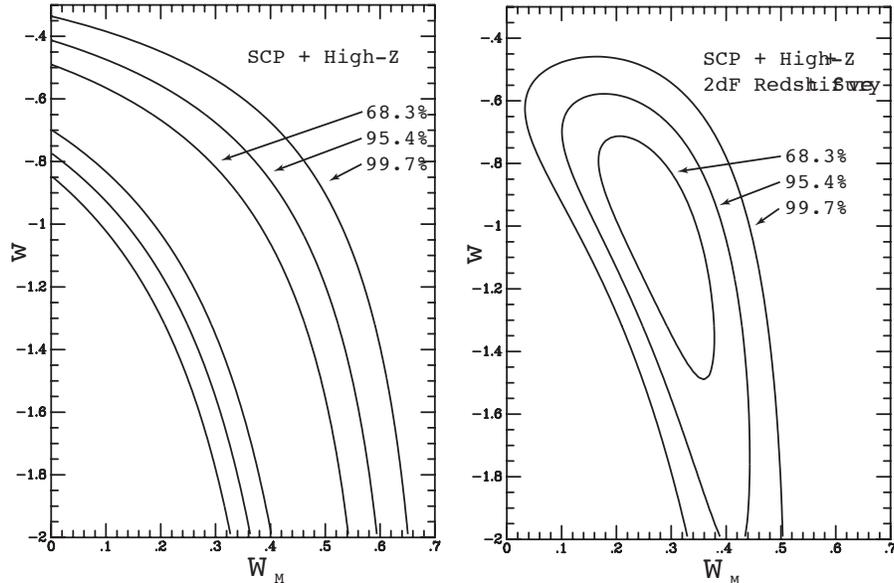
Fig. 6. Left panel: Contours of Ω_M versus w_x from current observational data. Right Panel: Contours of Ω_M versus w_x from current observational data, where the current value of Ω_M is obtained from the 2dF redshift survey. For both panels $\Omega_M + \Omega_x = 1$ is taken as a prior.

is spectacular, especially considering the two programs have worked in almost complete isolation from each other.

The easiest solution to explain the observed acceleration is to include an additional component of matter with an equation of state parameter more negative than $w < -1/3$; the most familiar being the cosmological constant ($w = -1$). Fig. 5 shows the joint confidence contours for values of Ω_M and Ω_Λ from both experiments. If we assume the Universe is composed only of normal matter and a cosmological constant, then with greater than 99.9% confidence the Universe has a non-zero cosmological constant or some other form of dark energy.

Of course, we do not know the form of dark energy which is leading to the acceleration, and it is worthwhile investigating what other forms of energy are possible additional components. Fig. 6 shows the joint confidence contours for the *HZSNS+SCP* observations for Ω_M and w_x (the equation of state of the unknown component causing the acceleration). Because this introduces an extra parameter, we apply the additional constraint that $\Omega_M + \Omega_x = 1$, as indicated by the *CMB* experiments [14]. The cosmological constant is preferred, but anything with a $w < -0.5$ is acceptable [23,77]. Additionally, we can add information about the value of Ω_M, as supplied by recent 2dF redshift survey results [98], as shown in the 2nd panel, where the constraint strengthens to $w < -0.6$ at 95% confidence [69].
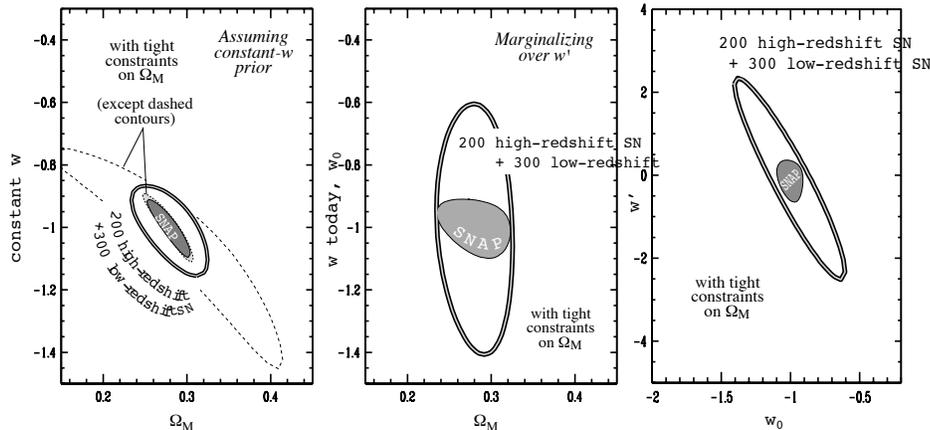
Fig. 7. Future expected constraints on dark energy: *Left panel:* Estimated 68% confidence regions for a constant equation of state parameter for the dark energy, w, versus mass density, for a ground-based study with 200 SNe between $z = 0.3 - 0.7$ (open contours), and for the satellite-based *SNAP* experiment with 2,000 SNe between $z = 0.3 - 1.7$ (filled contours). Both experiments are assumed to also use 300 SNe between $z = 0.02 - 0.08$. A flat cosmology is assumed (based on *Cosmic Microwave Background (CMB)* constraints) and the inner (solid line) contours for each experiment include tight constraints (from large scale structure surveys) on Ω_M, at the ± 0.03 level. For the *SNAP* experiment, systematic uncertainty is taken as $dm = 0.02(z/1.7)$, and for the ground-based experiment, $dm = 0.03(z/0.5)$. Such ground-based studies will test the hypothesis that the dark energy is in the form of a cosmological constant, for which $w = -1$ at all times. *Middle panel:* The same confidence regions for the same experiments not assuming the equation of state parameter, w, to be constant, but instead marginalizing over w', where $w(z) = w_0 + w'z$. (Weller and Albrecht [103] recommend this parameterization of $w(z)$ over the others that have been proposed to characterize well the current range of dark energy models.) Note that these planned ground-based studies will yield impressive constraints on the value of w today, w_0, even without assuming constant w. In fact, these constraints are comparable to the current measurements of w assuming it is constant (shown in the right panel of Fig. 6). *Right panel:* Estimated 68% confidence regions of the first derivative of the equation of state, w', versus its value today, w_0, for the same experiments.

6   The Future

How far can we push the SN measurements? Finding more and more SNe allows us to beat down statistical errors to arbitrarily small levels but, ultimately, systematic effects will limit the precision to which SNIa magnitudes can be applied to measure distances. Our best estimate is that it will be possible to control systematic effects from ground-based experiments to a level of ~ 0.03 mag. Carefully controlled ground-based experiments on 200 SNe will reach this statistical uncertainty in $z = 0.1$ redshift bins in the range $z = 0.3 - 0.7$, and

is achievable within five years. A comparable quality low redshift sample, with 300 SNe in $z = 0.02 - 0.08$, will also be achievable in that time frame [2].

The *SuperNova/Acceleration Probe (SNAP)* collaboration[1] has proposed to launch a dedicated cosmology satellite [1,68] – the ultimate SNIa experiment. This satellite will, if funded, scan many square degrees of sky, discovering well over a thousand SNIa per year and obtain their spectra and light curves out to $z = 1.7$. Besides the large numbers of objects and their extended redshift range, space-based observations will also provide the opportunity to control many systematic effects better than from the ground [21,53]. Fig. 7 shows the expected precision in the *SNAP* and ground-based experiments for measuring w, assuming a flat Universe. Perhaps the most important advance will be the first studies of the time variation of the equation of state w (see the right panel of Fig. 7 and [40,103]).

With rapidly improving *CMB* data from interferometers, the satellites *Microwave Anisotropy Probe (MAP)* and *Planck*, and balloon-based instrumentation planned for the next several years, *CMB* measurements promise dramatic improvements in precision on many of the cosmological parameters. However, the *CMB* measurements are relatively insensitive to the dark energy and the epoch of cosmic acceleration. SNIa are currently the only way to directly study this acceleration epoch with sufficient precision (and control on systematic uncertainties) that we can investigate the properties of the dark energy, and any time dependence in these properties. This ambitious goal will require complementary and supporting measurements of, for example, Ω_M from *CMB*, weak lensing, and large scale structure. The SN measurements will also provide a test of the cosmological results independent from these other techniques, which have their own systematic errors. Moving forward simultaneously on these experimental fronts offers the plausible and exciting possibility of achieving a comprehensive measurement of the fundamental properties of our Universe.

References

1. G. Aldering et al.: SPIE **4835**, 21 (2002)
2. G. Aldering et al.: SPIE **4836**, 93 (2002)
3. W.A. Baum: Astron. J. **62**, 6 (1957)
4. N. Benitez, A. Riess, P. Nugent, M. Dickinson, R. Chornock, A. Filippenko: Astrophys. J. Lett. **577**, L1 (2002)
5. M. Bessell: Pub. Astron. Soc. Pacific **102**, 1181 (1998)
6. D. Branch: In: *Encyclopedia of Astronomy and Astrophysics* (Academic, San Diego 1989) p. 733
7. D. Branch, G.A. Tammann: Ann. Rev. Astron. Astrophys. **30**, 359 (1992)
8. D. Branch, A. Fisher, P. Nugent: Astron. J. **106**, 2383 (1993)
9. D. Branch, A. Fisher, E. Baron, P. Nugent: Astrophys. J. Lett. **470**, L7 (1996)
10. D. Branch, S. Perlmutter, E. Baron, P. Nugent: In: *Resource Book on Dark Energy*, ed. by E.V. Linder (Snowmass 2001)
11. R. Cadonau: PhD Thesis, University of Basel (1987)

---

[1] See *http://snap.lbl.gov*

12. E. Cappellaro, M. Turatto, D.Yu. Tsvetkov, O.S. Bartunov, C. Pollas, R. Evans, M. Hamuy: Astron. Astrophys. **322**, 431 (1997)
13. P. Coles, F. Lucchin: In: *cosmology* (Wiley, Chicester 1995) p. 31
14. P. de Bernardis et al.: Nature **404**, 955 (2000)
15. R.G. Eastman, R.P. Kirshner: Astrophys. J. **347**, 771 (1989)
16. R.G. Eastman, B.P. Schmidt, R. Kirshner: Astrophys. J. **466**, 911 (1996)
17. A. Fisher, D. Branch, P. Hoeflich, A. Khokhlov: Astrophys. J. Lett. **447**, L73 (1995)
18. A.V. Filippenko: In: *SN1987A and Other Supernovae*, ed. by I.J. Danziger, K. Kjar (ESO, Garching 1991) p. 343
19. A.V. Fillipenko et al.: Astrophys. J. Lett. **384**, L15 (1992)
20. W.L. Freedman et al.: Astrophys. J. **553**, 47 (2001)
21. J. Frieman, D. Huterer, E.V. Linder, M.S. Turner: astro-ph 0208100 (2002)
22. P. Garnavich et al.: Astrophys. J. Lett. **493**, L53 (1998)
23. P. Garnavich et al.: Astrophys. J. **509**, 74 (1998)
24. L.G. Germany, A.G. Riess, B.P. Schmidt, N.B. Suntzeff: in preparation (2003)
25. G. Goldhaber et al.: In: *Thermonuclear Supernovae*, ed. by P. Ruiz-Lapuente, R. Canal, J. Isern (Aiguablava, June 1995; NATO ASI, 1997)
26. G. Goldhaber et al.: Astrophys. J. **558**, 359 (2001)
27. A. Goobar, S. Perlmutter: Astrophys. J. **450**, 14 (1995)
28. M. Hamuy, M.M. Phillips, J. Maza, M. Wischnjewsky, A. Uomoto, A.U. Landolt, R. Khatwani: Astron. J. **102**, 208 (1991)
29. M. Hamuy, M.M. Phillips, N.B. Suntzeff, R.A. Schommer, J. Maza, R. Aviles: Astron. J. **112**, 2391 (1996)
30. M. Hamuy, P.A. Pinto: Astron. J. **117**, 1185 (1999)
31. M. Hamuy et al.: Astron. J. **106**, 2392 (1993)
32. M. Hamuy et al.: Astron. J. **109**, 1 (1995)
33. M. Hamuy et al.: Astron. J. **112**, 2408 (1996)
34. M. Hamuy et al.: Astrophys. J. **558**, 615 (2001)
35. L. Hansen, H.E. Jorgensen, H.U. Nørgaard-Nielsen, R.S. Ellis, W.J. Couch: Astron. Astrophys. **211**, L9 (1989)
36. R.P. Harkness, J.C. Wheeler: In: *Supernovae*, ed. by A.G. Petschek (Springer-Verlag, New York 1990) p. 1
37. D.E. Holz, R.M. Wald: Phys. Rev. D **58**, 063501 (1998)
38. D.E. Holz: Astrophys. J. **506**, 1 (1998)
39. M.L. Humason, N.U. Mayall, A.R. Sandage: Astrophys. J. **61**, 97 (1956)
40. D. Huterer, M.S. Turner: Phys. Rev. D **64**, 123527 (2001)
41. S. Jha: PhD Thesis, Harvard University (2002)
42. C.T. Kowal: Astron. J. **73**, 1021 1968
43. A. Kim, A. Goobar, S. Perlmutter: Pub. Astron. Soc. Pacific **108**, 190 (1996)
44. R.P. Kirshner, J. Kwan: Astrophys. J. **193**, 27 (1974)
45. R. Kantowski, T. Vaughan, D. Branch: Astrophys. J. **447**, 35 (1995)
46. B. Leibundgut: PhD Thesis, University of Basel (1988)
47. B. Leibundgut, G.A. Tammann: Astron. Astrophys. **230**, 81 (1990)
48. B. Leibundgut, G.A. Tammann, R. Cadonau, D. Cerrito: Astron. Astrophys. Suppl. Ser. **89**, 537 (1991)
49. B. Leibundgut et al.: Astron. J. **105**, 301 (1993)
50. B. Leibundgut et al.: Astrophys. J. Lett. **466**, L21 (1996)
51. D.C. Leonard, A.V. Filippenko, D.R. Ardila, M.S. Brotherton: Astrophys. J. **553**, 861 (2001)

52. D.C. Leonard et al.: Pub. Astron. Soc. Pacific **114**, 35 (2002)
53. E. Linder, D. Huterer: astro-ph 0208138 (2002)
54. D.L. Miller, D. Branch: Astron. J. **100**, 530 (1990)
55. E. Mortsell, C. Gunnarsson, A. Goobar: Astrophys. J. **561**, 106 (2001)
56. R.A. Muller, H.J.M. Newberg, C.R. Pennypacker, S. Perlmutter, T.P. Sasseen, C.K. Smith: Astrophys. J. Lett. **384**, L9 (1992)
57. H.U. Nørgaard-Nielsen, L. Hansen, H.E. Jorgensen, A. Aragon Salamanca, R.S. Ellis: Nature **339**, 523 (1989)
58. P. Nugent, A. Kim, S. Perlmutter: Pub. Astron. Soc. Pacific **114**, 803 (2002)
59. N. Panagia: In: *Supernovae as Distance Indicators*, ed. by N. Bartel, (Springer-Verlag, Berlin 1985) p. 14
60. R. Pain et al.: Astrophys. J. **473**, 356 (1996)
61. R. Pain et al.: Astrophys. J. **577**, 120 (2002)
62. G. Pearce, B. Patchett, J. Allington-Smith, I. Parry: Astrophys. Space Sci. **150**, 267 (1988)
63. M.M. Phillips et al.: Pub. Astron. Soc. Pacific **99**, 592 (1987)
64. M.M. Phillips: Astrophys. J. Lett. **413**, L105 (1993)
65. M.M. Phillips, P. Lira, N.B. Suntzeff, R.A. Schommer, M. Hamuy, J. Maza: Astron. J. **118**, 1766 (1999)
66. P.J.E. Peebles: In: *Principles of Physical cosmology* (Princeton University Press, Princeton 1993)
67. S. Perlmutter, R.A. Muller, H.J.M. Newberg, C.R. Pennypacker, T.P. Sasseen, C.K. Smith: ASP Conf. Proc. **34**, 67 (1992)
68. S. Perlmutter, E. Linder: In *Dark Matter 2002, Proc. 5th International UCLA Symposium on Sources and Detection of Dark Matter and Dark Energy in the Universe*, ed. by D.B. Cline (Elsevier, Amsterdam 2003)
69. S. Perlmutter, M. Turner, M. White: Phys. Rev. Lett. **83**, 670 (1999)
70. S. Perlmutter et al.: IAUC 5956 (1994)
71. S. Perlmutter et al.: IAUC 6263 (1995)
72. S. Perlmutter et al.: IAUC 6270 (1995)
73. S. Perlmutter et al.: Astrophys. J. Lett. **440**, L41 (1995)
74. S. Perlmutter et al.: Astrophys. J. **483**, 565 (1997)
75. S. Perlmutter et al.: Nature **391**, 51 (1998)
76. S. Perlmutter et al.: In: *Thermonuclear Supernovae*, ed. by P. Ruiz-Lapuente, R. Canal, J. Isern (Aiguablava, June 1995; NATO ASI, 1997)
77. S. Perlmutter et al.: Astrophys. J. **517**, 565 (1999)
78. M.M. Phillips, L.A. Wells, N.B. Suntzeff, M. Hamuy, B. Leibundgut, R.P. Kirshner, C.B. Foltz: Astron. J. **103**, 1632 (1992)
79. A.G. Riess, W.H. Press, R.P. Kirshner: Astrophys. J. **473**, 88 (1996)
80. A.G. Riess, P. Nugent, A.V. Filippenko, R.P. Kirshner, S. Perlmutter: Astrophys. J. **504**, 935 (1998)
81. A.G. Riess, A.V. Filippenko, W. Li, B.P. Schmidt: Astron. J. **118**, 2668 (1999)
82. A.G. Riess et al.: Astron. J. **114**, 722 (1997)
83. A.G. Riess et al.: Astron. J. **116**, 1009 (1998)
84. A.G. Riess et al.: Astron. J. **117**, 707 (1999)
85. A.G. Riess et al.: Astrophys. J. **560**, 49 (2001)
86. B.P. Schmidt, R.P. Kirshner, R.G. Eastman, M.M. Phillips, N.B. Suntzeff, N.B. Hamuy, J. Maza, R. Aviles: Astrophys. J. **432**, 42 (1994)
87. B. Schmidt et al.: Astrophys. J. **507**, 46 (1998)
88. A. Saha, A. Sandage, G.A. Tammann, A.E. Dolphin, J. Christensen, N. Panagia, F.D. Macchetto: Astrophys. J. **562**, 313 (2001)

89. D.J. Schlegel, D.P. Finkbeiner, M. Davis: Astrophys. J. Suppl. **500**, 525 (1998)
90. A. Sandage, G.A. Tammann: Astrophys. J. **415**, 1 (1993)
91. M. Sullivan et al.: Mon. Not. R. Astron. Soc.   , in press (2003)
92. G.A. Tammann, B. Leibundgut: Astron. Astrophys. **236**, 9 (1990)
93. G.A. Tammann, A. Sandage: Astrophys. J. **452**, 16 (1995)
94. A. Uomoto, R.P. Kirshner: Astron. Astrophys. **149**, L7 (1985)
95. S. van den Bergh: Astrophys. J. Lett. **453**, L55 (1995)
96. S. van den Bergh, J. Pazder: Astrophys. J. **390**, 34 (1992)
97. T.E. Vaughan, D. Branch, D.L. Miller, S. Perlmutter: Astrophys. J. **439**, 558 (1995)
98. L. Verde et al.: Mon. Not. R. Astron. Soc. **335**, 432 (2002)
99. R.V. Wagoner: Astrophys. J. Lett. **250**, L65 (1981)
100. J. Wambsgabss, R. Cen, X. Guohong, J. Ostriker: Astrophys. J. Lett. **475**, L81 (1997)
101. L. Wang, A.D. Howell, P. Höflich, J.C. Wheeler: Astrophys. J. **550**, 1030 (2001)
102. J.C. Wheeler, R. Levreault: Astrophys. J. Lett. **294**, L17 (1985)
103. J. Weller, A. Albrecht: Phys. Rev. D **65**, 103512 (2002)
104. D.M. Wittman, J.A. Tyson, G.M. Bernstein, R.W. Lee, I.P. dell'Antonio, P. Fischer, D.R. Smith, M.M. Blouke: SPIE **3355**, 626 (1998)